JACS
JOURNAL OF THE AMERICAN CHEMICAL SOCIETY
Article
pubs.acs.org/JACS

Phosphate-Catalyzed Degradation of D-Glucosone in Aqueous Solution Is Accompanied by C1−C2 Transposition

Wenhui Zhang and Anthony S. Serianni*

Department of Chemistry and Biochemistry, University of Notre Dame, Notre Dame, Indiana 46556, United States

Supporting Information

ABSTRACT: Pathways in the degradation of the C_6 1,2-dicarbonyl sugar (osone) D-glucosone **2** (D-*arabino*-hexos-2-ulose) in aqueous phosphate buffer at pH 7.5 and 37 °C have been investigated by ^{13}C and ^{1}H NMR spectroscopy with the use of singly and doubly ^{13}C-labeled isotopomers of **2**. Unlike its 3-deoxy analogue, 3-deoxy-D-glucosone (3-deoxy-D-*erythro*-hexos-2-ulose) (**1**), **2** does not degrade via a 1,2-hydrogen shift mechanism but instead initially undergoes C1−C2 bond cleavage to yield D-ribulose **3** and formate. The latter bond cleavage occurs via a 1,3-dicarbonyl intermediate initially produced by enolization at C3 of **2**. However, a careful monitoring of the fates of the sketetal carbons of **2** during its conversion to **3** revealed unexpectedly that C1−C2 bond cleavage is accompanied by C1−C2 transposition in about 1 out of every 10 transformations. Furthermore, the degradation of **2** is catalyzed by inorganic phosphate (P_i), and by the P_i-surrogate, arsenate. C1−C2 transposition was also observed during the degradation of the C_5 osone, D-xylosone (D-*threo*-pentose-2-ulose), showing that this transposition may be a common feature in the breakdown of 1,2-dicarbonyl sugars bearing an hydroxyl group at C3. Mechanisms involving the reversible formation of phosphate adducts to **2** are proposed to explain the mode of P_i catalysis and the C1−C2 transposition. These findings suggest that the breakdown of **2** in vivo is probably catalyzed by P_i and likely involves C1−C2 transposition.

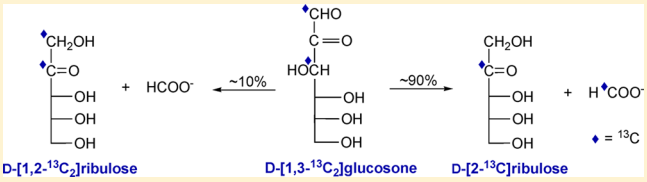

INTRODUCTION

The current global diabetes epidemic[1] has spurred renewed interest in combating this debilitating disease that afflicts both young and old. Current therapeutic approaches range from better monitoring and control of blood glucose concentrations to gene replacement and stem cell therapies to restore aberrant insulin production and/or glucose transport.[2−4] The elevated glucose concentrations in the blood and tissues of diabetic patients cause covalent modification of proteins through the process of glycation, the spontaneous, non-enzyme-catalyzed reaction of the acyclic (*aldehydo*) form of glucose with lysine side chains to initially form Schiff bases.[5] The latter undergo spontaneous rearrangement to form protein-bound Amadori adducts, a process that is considered the committed (i.e., irreversible) step in protein glycation.[6]

The biochemical fates of Amadori adducts are still a matter of debate, but it is commonly assumed that C−C bond fragmentation in these adducts, or in their oxidized derivatives, produces reactive oxygen species (ROS) which inflict oxidative damage to proteins and other structures in their vicinity.[7] This damage is largely responsible for the multiple negative biological consequences of glycation.

Glycation reduces the biological activities of proteins and enzymes, especially those with long lifetimes.[8] Thus, in addition to the treatment strategies mentioned above, efforts have been made to develop therapies that reduce glycation in vivo and/or prevent the degradation of Amadori adducts to ROS. For example, the B_6 vitamer, pyridoxamine, appears to reduce the detrimental effects of glycation in diabetic patients,[9] although side effects from this treatment have been reported.[10]

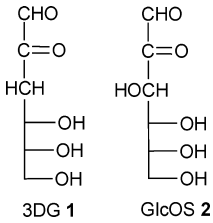

In addition to the primary reaction between glucose and proteins in vivo, secondary reactions also occur. Glucose spontaneously rearranges and/or degrades in buffered (phosphate) aqueous solution at pH 7.5, and the byproduct reactive carbon species (RCS; e.g., methyl glyoxal and glyoxal) from this degradation (autoxidation) in vivo may inflict greater tissue damage than glucose itself.[11] Among the potential rearrangement products are the 1,2-dicarbonyl sugars (osones), 3-deoxy-D-glucosone (3-deoxy-D-*erythro*-hexos-2-ulose; 3DG; **1**) and D-glucosone (D-*arabino*-hexos-2-ulose; GlcOS; **2**). 3DG is produced in vivo by spontaneous (nonenzymic) reaction of D-glucose with protein (Lys side chains) to give an initial aldimine (Schiff base), which rearranges in several steps to liberate free 3DG (Scheme 1).[12] The same initial Schiff base also partitions into the competing Amadori pathway (Scheme S1, Supporting Information). Other pathways for the formation

Received: February 29, 2012
Published: May 31, 2012

   dx.doi.org/10.1021/ja3020296 | J. Am. Chem. Soc. 2012, 134, 11511−11524

Scheme 1

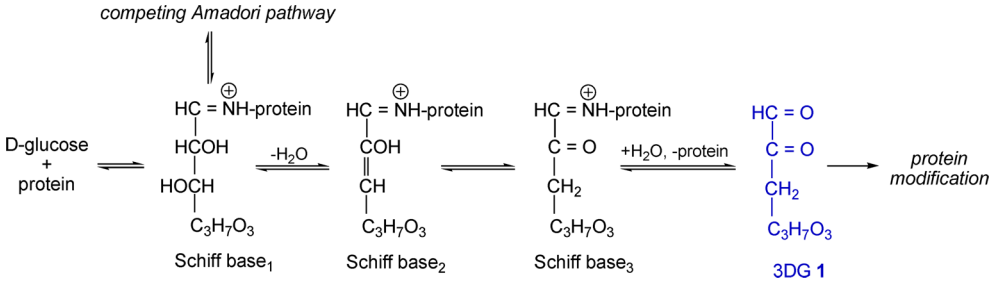

of **1** in vivo are also possible.[13,14] The production of **2** in vivo may not be protein-mediated but rather initiates from D-glucose, which rearranges to the 1,2-enediol, with subsequent oxidation giving **2** (Scheme 2).[12] Recent studies suggest that **2** may also form in vivo from the cleavage of Amadori products mediated by peroxynitrite.[15]

Scheme 2

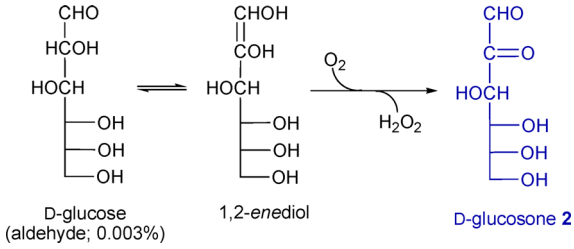

We showed recently that **1** rearranges in aqueous phosphate buffer at pH 7.5 and 37 °C to give two major products, 3-deoxy-D-*ribo*-hexonic acid and 3-deoxy-D-*arabino*-hexonic acid.[16] Deuterium and ^{13}C-labeling experiments revealed that this rearrangement occurs through an intramolecular 1,2-hydrogen transfer mechanism.[17] Competing with this skeletal rearrangement at a lower level is C1−C2 bond cleavage, which yields formate and 2-deoxy-D-ribonate.[16]

Degradation studies of **1** led to the question posed in the present work: Does the 3DG analogue, D-glucosone **2**, degrade in aqueous phosphate buffer in a manner similar to that found for **1**? We show in this report, through the use of ^{13}C-labeled isotopomers of GlcOS ($\mathbf{2}^1$, $\mathbf{2}^2$, $\mathbf{2}^{1,2}$ and $\mathbf{2}^{1,3}$; superscripts denote labeled carbons) and NMR that replacement of the CH_2 group at C3 of **1** by a HCOH group affects the degradation route significantly. Furthermore, the degradation of **2** is accompanied by an unexpected transposition of the C1−C2 fragment via a mechanism mediated by inorganic phosphate.

EXPERIMENTAL METHODS

A. Reagents. D-[1-^{13}C]Glucose, D-[2-^{13}C]glucose, D-[1,2-$^{13}C_2$]-glucose, D-[1,3-$^{13}C_2$]glucose, D-[1-^{13}C]xylose, D-[1-^{13}C]ribulose $\mathbf{3}^1$, and DL-[1-^{13}C]glyceraldehyde $\mathbf{4}^1$ were obtained from Omicron Biochemicals, Inc. (South Bend, IN).

B. Synthesis of ^{13}C-Labeled D-Glucosones 2 and D-Xylosone 5. Four ^{13}C isotopomers of GlcOS **2** were prepared: D-[1-^{13}C]-glucosone ($\mathbf{2}^1$), D-[2-^{13}C]glucosone ($\mathbf{2}^2$), D-[1,2-$^{13}C_2$]glucosone ($\mathbf{2}^{1,2}$), and D-[1,3-$^{13}C_2$]glucosone ($\mathbf{2}^{1,3}$). The synthetic route for their preparation (Scheme S2, Supporting Information) involved treatment of ^{13}C-labeled D-glucoses with pyranose 2-oxidase (glucose 2-oxidase, PROD, EC 1.1.3.10; Sigma).[16,18,19] Labeled D-glucose (200 mg, 1.11 mmol) was dissolved in deionized water (60 mL) in a 250-mL three-neck flask, and PROD (5.8 mg) and catalase (2.0 mg; Sigma) were added. The solution was stirred gently at 25 °C and aerated (compressed air, ~20 mL/min), and the solution pH was maintained at 7.0 with periodic additions of 0.01 N NaOH until the pH stopped dropping (~3 h). The reaction mixture was then filtered though a 0.2 μm membrane filter, and the filtrate was concentrated at 30 °C in vacuo. The solution was applied to a chromatographic column (2.5 × 110 cm) containing Dowex 50 × 8 (200−400 mesh) ion-exchange resin in the Ca^{2+} form.[20] The column was eluted with distilled, decarbonated water at ~1.5 mL/min, and fractions (12 mL) were collected and assayed by TLC (silica gel; spots detected by charring after spraying with 1% (*w*/*v*) $CeSO_4$−2.5% (*w*/*v*) $(NH_4)_6Mo_7O_{24}$−10% aq H_2SO_4 reagent).[21] Fractions nos. 22−29 containing osone **2** were pooled and concentrated at 30 °C in vacuo. The product **2** (168 mg, 0.94 mmol, 85% yield) was identified by its characteristic ^{13}C

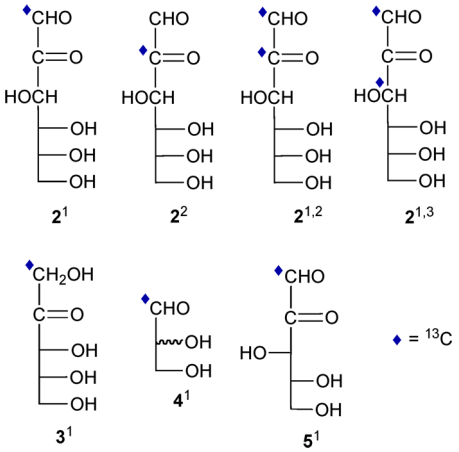

chemical shifts,[22] and purity was >95% based on ^{13}C NMR assay. Aqueous solutions of **2** were stored at 4 °C prior to use.

D-[1-^{13}C]Xylosone $\mathbf{5}^1$ (D-[1-^{13}C]*threo*-pentos-2-ulose) was prepared from D-[1-^{13}C]xylose as described previously by Vuorinen and Serianni.[23]

C. General Procedure Used in Degradation Studies of 2 by NMR. The ^{13}C-labeled D-glucosone ($\mathbf{2}^1$, $\mathbf{2}^2$, $\mathbf{2}^{1,2}$, or $\mathbf{2}^{1,3}$) was dissolved in 100 mM sodium phosphate buffer at pH 7.5 to give a 10−20 mM solution in **2** containing sodium azide (about 0.2 mg/mL solution) and ^2H_2O (10% *v*/*v*), and the resulting solution was incubated at 37 °C in the dark. NMR spectra of the reaction mixture were obtained periodically by withdrawing an aliquot from the reaction mixture and transferring it into a 5-mm NMR tube. NMR spectra were collected at 22 °C on a 600 MHz FT-NMR spectrometer as described below.

D. NMR Spectroscopy. High-resolution 1D ^1H and $^{13}C\{^1H\}$ NMR spectra of reaction mixtures were obtained at 22 °C. Samples were analyzed in 5-mm NMR tubes on a 600-MHz FT-NMR spectrometer equipped with a 5 mm ^1H−$^{19}F/^{15}N$−^{31}P dual broadband probe. ^1H NMR spectra (600 MHz) were typically collected with a ~7000 Hz spectral window and a ~3.5 s recycle time. $^{13}C\{^1H\}$ NMR spectra (150 MHz) were collected with ~37 000 Hz spectral windows and ~3.0 s recycle times. FIDs were processed to optimize spectral S/N, and final spectra had digital resolutions of ~0.05 Hz/pt for ^1H

dx.doi.org/10.1021/ja3020296 | J. Am. Chem. Soc. 2012, 134, 11511−11524

NMR and ~0.14 Hz/pt for ^{13}C NMR. Chemical shifts were referenced externally to sodium 4,4-dimethyl-4-silapentane-1-sulfonate (DSS).

RESULTS AND DISCUSSION

A. Degradation of D-[2-^{13}C]Glucosone 2^2. Testing for the Formation of D-[1-^{13}C]Ribulose 3^1. Prior studies reported by Baynes and co-workers[24] have shown that **2** degrades in aqueous phosphate buffer (200 mM, pH 7.4, 37 °C) to give D-ribulose **3** in 20% yield and other unidentified products. A reasonable mechanism for the formation of **3**^{1} from **2**^{2} is shown in Scheme 3; C1−C2 bond cleavage in the presumed 1,3-dicarbonyl intermediate is promoted by OH^- attack on C1 to give unlabeled formate as the second product.

Scheme 3

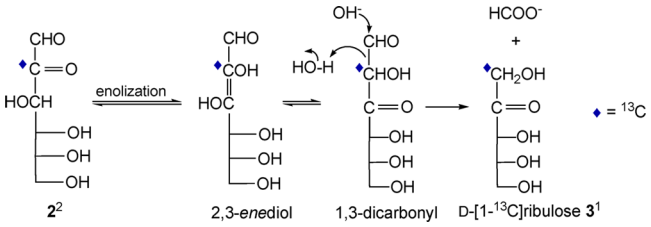

To test the mechanism in Scheme 3, **2**^{2} was incubated in 100 mM Na-phosphate buffer, pH 7.5, at 37 °C, and aliquots were withdrawn from the reaction vessel for assay by $^{13}C\{^1H\}$ NMR. The $^{13}C\{^1H\}$ NMR spectrum obtained after 1 day is shown in Figure 1. The downfield region contained three weak signals arising from D-[1-^{13}C]arabinonate **6**^{1} (181.87 ppm), [^{13}C]-formate (173.62 ppm), and [^{13}C]bicarbonate (162.89 ppm). The anomeric region contained signals from unreacted **2**^{2} (103.41, 99.99, 96.29, and 95.72 ppm), and the upfield region contained only signals[25] arising from D-[1-^{13}C]ribulose **3**^{1} (69.10, 65.45, and 65.19 ppm). After 15 days of reaction (Figure 2), an additional downfield signal was observed from [1-^{13}C]glycolate **7**^{1} (182.48 ppm) (this signal first appeared after ~2 days of reaction; data not shown). The anomeric region was virtually devoid of signals from unreacted **2**^{2}, but D-[1-^{13}C]ribose **8**^{1} (103.58, 98.91, 96.45, and 96.16 ppm) and D-[1-^{13}C]arabinose **9**^{1} (99.44 and 95.24 ppm) were detected,[26] with the former in greater abundance. The upfield region contained signals from D-[1-^{13}C]ribulose **3**^{1}, D-[1-^{13}C]xylulose **10**^{1} (68.63 and 65.13 ppm), and [2-^{13}C]glycolate **7**^{2} (63.89 ppm). After 50 days of reaction (Figure S1, Supporting Information), only signals from [1-^{13}C]glycolate **7**^{1}, [^{13}C]-formate, and [1-^{13}C]arabinonate **6**^{1} were detected downfield, and the anomeric carbon region showed new weak signals[26] from D-[1-^{13}C]lyxose **11**^{1} (96.73 ppm) in addition to those arising from D-[1-^{13}C]ribose **8**^{1} and D-[1-^{13}C]arabinose **9**^{1}. The strong upfield signal at 63.88 ppm arises from [1-^{13}C]glycolate **7**^{1}.

Studies of **2**^{2} confirm the production of D-[1-^{13}C]ribulose **3**^{1}, a result consistent with the mechanism shown in Scheme 3. In addition, D-[1-^{13}C]arabinonate **6**^{1} is detected as a degradation product, with C1 of **2**^{2} presumably lost as unlabeled formate (Scheme 4). Unexpectedly, $H^{13}COO^-$ is detected *early* in the degradation of **2**^{2}, and glycolate **7** is detected with ^{13}C-labeling at either C1 or C2. D-[1-^{13}C]Ribose **8**^{1}, D-[1-^{13}C]arabinose **9**^{1}, D-[1-^{13}C]xylulose **10**^{1}, and D-[1-^{13}C]lyxose **11**^{1} presumably arise from the D-[1-^{13}C]ribulose **3**^{1} intermediate via isomerization and epimerization.

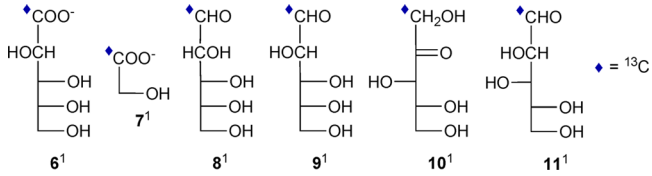

Additional insight into the degradation of **2**^{2} was obtained by investigating the behavior of authentic D-[1-^{13}C]ribulose **3**^{1} when incubated under reaction conditions similar to those used in the degradation of **2**^{2}. $^{13}C\{^1H\}$NMR spectra of the reaction solution after 1 day at room temperature, followed by 2 days and 10 days at 37 °C, are shown in Figure S2 (Supporting Information). These data show that the unidentified intermediates (very weak signals at ~62 ppm) in Figures 2D and S1D apparently arise from the degradation of the D-

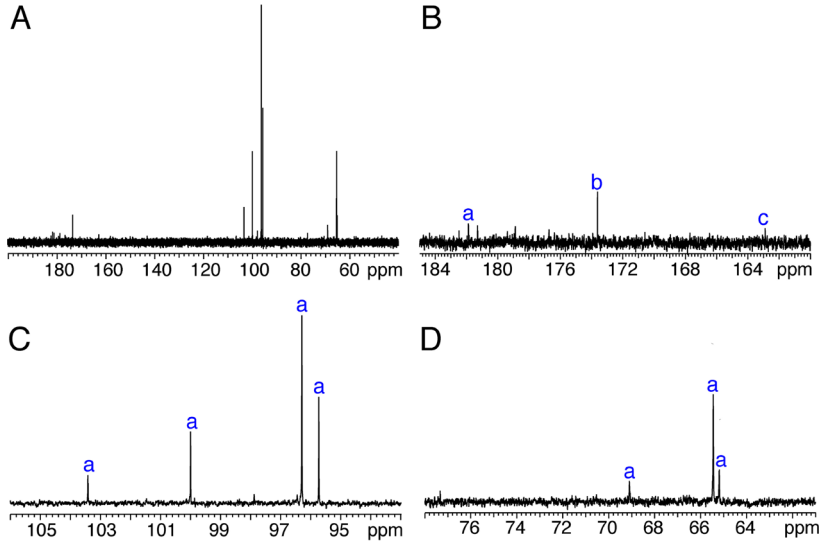

Figure 1. The $^{13}C\{^1H\}$ NMR spectrum of the reaction mixture with **2**^{2} (100 mM NaP_i; pH 7.5; 37 °C) after 1 day. (A) Full spectrum. (B) Downfield region showing signals from [1-^{13}C]arabinonate **6**^{1} (a), $H^{13}COO^-$ (b), and $H^{13}CO_3^-$ (c). (C) The anomeric carbon region showing signals (a) from unreacted **2**^{2}. (D) Upfield region showing signals (a) from D-[1-^{13}C]ribulose **3**^{1} (α- and β-furanose and keto forms).[25]

dx.doi.org/10.1021/ja3020296 | J. Am. Chem. Soc. 2012, 134, 11511−11524

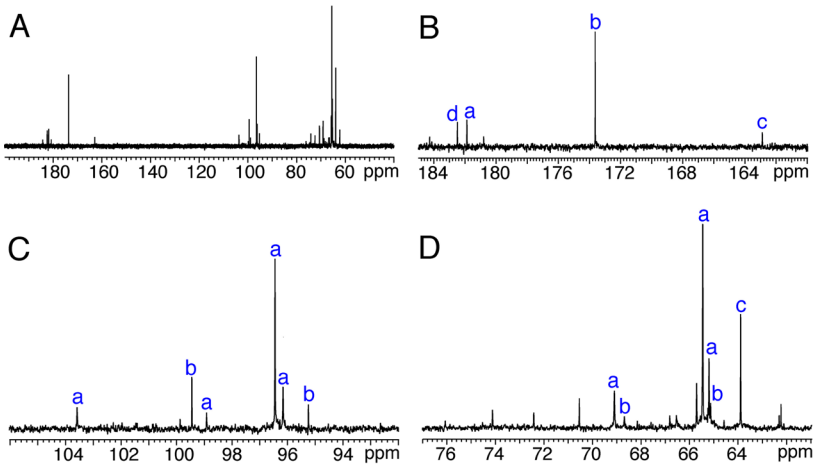

Figure 2. The $^{13}C\{^1H\}$ NMR spectrum of the reaction mixture with **2**^{2} (100 mM NaP_i; pH 7.5; 37 °C) after 15 days. (A) Full spectrum. (B) Downfield region showing signals from D-[1-^{13}C]arabinonate **6**^{1} (a), $H^{13}COO^-$ (b), $H^{13}CO_3^-$ (c), and [1-^{13}C]glycolate **7**^{1} (d). (C) The anomeric carbon region showing signals from D-[1-^{13}C]ribose **8**^{1} (a) and D-[1-^{13}C]arabinose **9**^{1} (b). (D) Upfield region showing signals from D-[1-^{13}C]ribulose **3**^{1} (α- and β-furanose and keto forms) (a),[25] D-[1-^{13}C]xylulose **10**^{1} (b), and [2-^{13}C]glycolate **7**^{2} (c).

Scheme 4

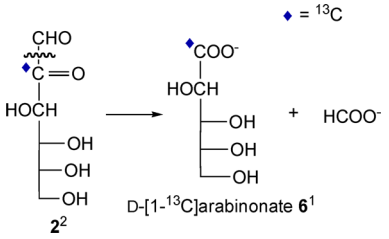

Scheme 5

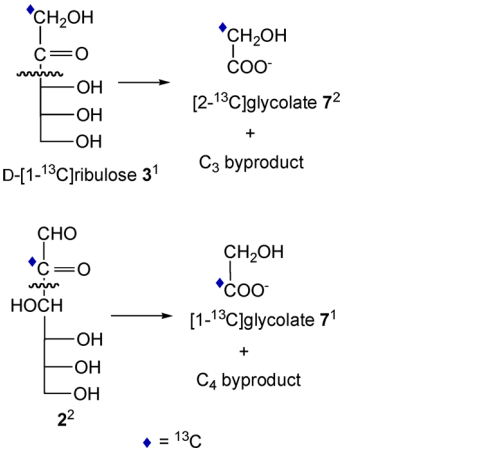

ribulose intermediate. Furthermore, after an extended reaction period, only [^{13}C]bicarbonate and [2-^{13}C]glycolate **7**^{2} were observed; signals from the intermediates at ~62 ppm eventually disappear.

The formation of labeled products other than D-[1-^{13}C]-ribulose **3**^{1} generated from **2**^{2} during degradation leads to questions about the overall course of the reaction. How does the [^{13}C]formate produced early in the reaction arise? [2-^{13}C]Glycolate **7**^{2} arises presumably from the degradation of the D-[1-^{13}C]ribulose **3**^{1} intermediate, while [1-^{13}C]glycolate **7**^{1} may arise from direct C2−C3 bond cleavage of **2**^{2} (Scheme 5). Degradation studies of D-[1-^{13}C]glucosone **2**^{1} were therefore undertaken to investigate these proposed transformations.

B. Degradation of D-[1-^{13}C]Glucosone 2^1. The $^{13}C\{^1H\}$ NMR spectrum of the reaction mixture after 1 day of degradation of **2**^{1} is shown in Figure 3. The strong downfield signal at 173.62 ppm arises from [^{13}C]formate ($H^{13}COO^-$), presumably generated by C1−C2 bond cleavage in **2**^{1} via routes shown in Schemes 3 and 4. The anomeric carbon region (Figure 3C) contained four intense signals arising from unreacted **2**^{1} (97.70, 97.27, 92.70, and 92.03 ppm) and several weaker unassigned signals. Importantly, several upfield signals between 62 and 66 ppm were observed, and two of these were assigned to the α- and β-furanose forms of D-[1-^{13}C]ribulose **3**^{1} (65.45 and 65.19 ppm) and a third to [2-^{13}C]glycolate **7**^{2} (63.89 ppm). The closely spaced signals at ~62 ppm (62.35, 62.25, and 62.24 ppm) are similar to the very weak signals observed during the degradation of **2**^{2} (Figures 2D and S1D), which were shown to arise during the degradation of **3**^{1} (Figure S2). After 15 days, the strong signal arising from $H^{13}COO^-$ was still observed (Figure 4A and 4B), but no signals from unreacted **2**^{1} were detected (Figure 4C). Anomeric carbon signals, however, were observed for D-[1-^{13}C]ribose **8**^{1} and D-[1-^{13}C]arabinose **9**^{1}. The upfield region showed the presence of D-[1-^{13}C]ribulose **3**^{1} (69.09, 65.46, and 65.19 ppm) and [2-^{13}C]glycolate **7**^{2}, although the latter contributed the dominant signal in this region, in contrast to the results obtained after 1 day (Figure 3D). This enhancement appears to come at the expense of the unidentified intermediates, whose signals are dominant in Figure 3D but relatively weak in Figure 4D.

The above NMR results with **2**^{1} as reactant show that, unlike the degradation of 3-deoxy-D-glucosone **1**,[17] degradation involving an intramolecular 1,2-hydrogen shift (benzylic acid rearrangement) is not favored for **2**, based on the absence of carboxylate (C1) carbon signals attributable to D-[1-^{13}C]-gluconate **12**^{1} and D-[1-^{13}C]mannonate **13**^{1} in Figures 3 and 4 (Scheme 6). The detection of $H^{13}COO^-$ supports the occurrence of C1−C2 bond cleavage in **2**^{1}, yielding unlabeled D-arabinonate as shown in Scheme 4.

During the degradation of **2**^{1}, intermediate D-ribulose **3** is produced with ^{13}C-labeling at C1, an unexpected result inconsistent with the route shown in Scheme 3 (i.e., when **2**^{1} is the reactant, **3** should be unlabeled). The detection of **3**^{1}

dx.doi.org/10.1021/ja3020296 | J. Am. Chem. Soc. 2012, 134, 11511−11524

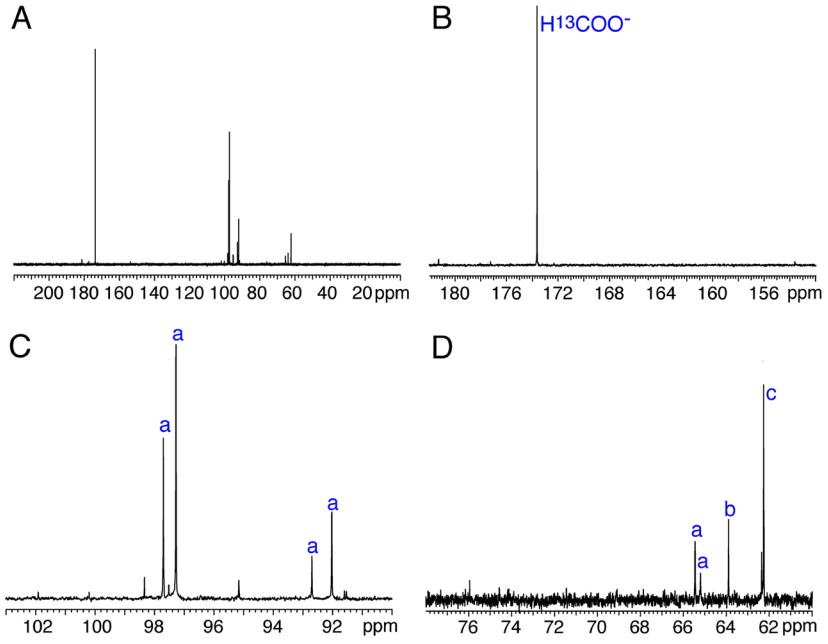

Figure 3. The $^{13}C\{^{1}H\}$ NMR spectrum of the reaction mixture with **2**[1] (100 mM NaP_i; pH 7.5; 37 °C) after 1 day. (A) Full spectrum. (B) Downfield region showing the intense $H^{13}COO^-$ signal. (C) The anomeric carbon region showing signals (a) from unreacted **2**[1]. (D) Upfield region showing signals from D-[1-^{13}C]ribulose **3**[1] (α- and β-furanose forms) (a), [2-^{13}C]glycolate (b), and unidentified intermediates (c).

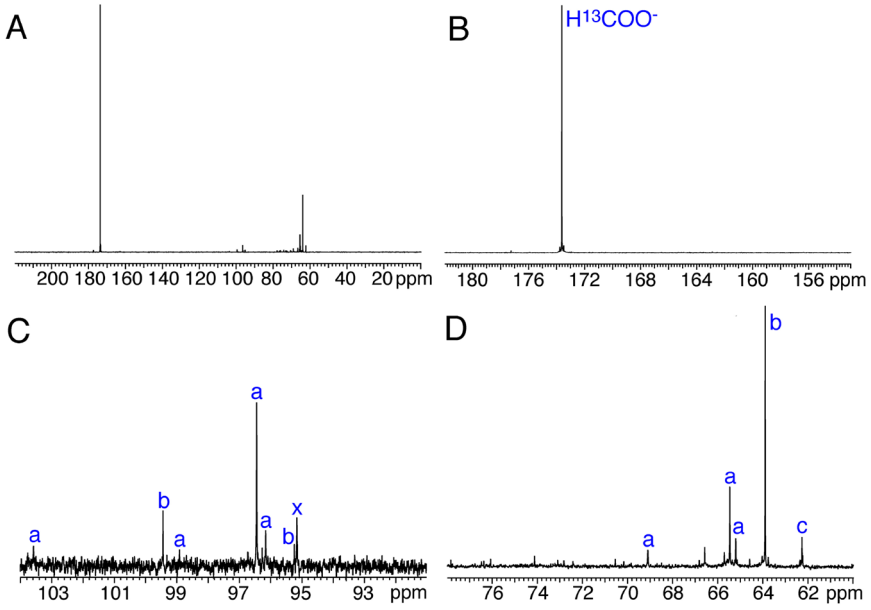

Figure 4. The $^{13}C\{^{1}H\}$ NMR spectrum of the reaction mixture with **2**[1] (100 mM NaP_i; pH 7.5; 37 °C) after 15 days. (A) Full spectrum. (B) Downfield region showing the intense signal from $H^{13}COO^-$. (C) The anomeric carbon region showing signals from D-[1-^{13}C]ribose **8**[1] (a), D-[1-^{13}C]arabinose **9**[1] (b), and an unidentified species (x) . (D) Upfield region showing signals from D-[1-^{13}C]ribulose **3**[1] (α- and β-furanose and keto forms) (a), [2-^{13}C]glycolate **7**[2] (b), and unidentified intermediates (c).

Scheme 6

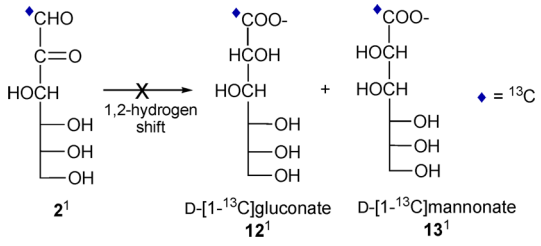

suggests that C1−C2 bond cleavage in **2** may be preceded by C1−C2 transposition. If this transposition had occurred during the degradation of **2**[2] (see above), the unlabeled D-ribulose **3** that formed (in addition to **3**[1]) would not be observed easily in the spectrum, because the ^{13}C NMR assay detects only those carbons that are ^{13}C-labeled (i.e., the concentration of unlabeled **3** is too low to be observed).

The detection of [2-^{13}C]glycolate **7**[2] during the degradation of **2**[1] is consistent with a route involving C2−C3 cleavage, as shown in Scheme 5. If C1−C2 transposition occurred prior to cleavage and degradation, then a portion of the [2-^{13}C]glycolate

dx.doi.org/10.1021/ja3020296 | J. Am. Chem. Soc. 2012, 134, 11511−11524

pool could be produced from the intermediate D-[1-^{13}C]-ribulose **3**^{1} (Scheme 5); the coexistence of both pathways is only implied from these data based on the detection of **3**^{1} in the reaction mixture.

The generation of D-[1-^{13}C]ribose **8**^{1} and D-[1-^{13}C]arabinose **9**^{1} (Figure 4C) presumably occurs by isomerization of **3**^{1} to the corresponding C2-epimeric aldopentoses via a 1,2-enediol intermediate. The detection of **8**^{1} and **9**^{1} thus provides additional indirect evidence for the production of D-[1-^{13}C]-ribulose **3**^{1} during the degradation of **2**^{1}.

The production of D-[1-^{13}C]ribulose **3**^{1} and [^{13}C]formate during the degradation of both **2**^{1} and **2**^{2} must be accompanied by the formation of unlabeled **3** and unlabeled formate if C1−C2 transposition occurred during degradation. The unlabeled fraction of these pools would not be detected by ^{13}C NMR given their low concentrations in solution. Because detection of these unlabeled components would provide confirmatory evidence for the proposed C1−C2 transposition, **2**^{1} and **2**^{2} were separately incubated in 100 mM phosphate buffer at pH 7.5 and 37 °C for 3 days, and the formate pools were analyzed in the resulting solutions by ^{1}H NMR (Figure 5). The formate

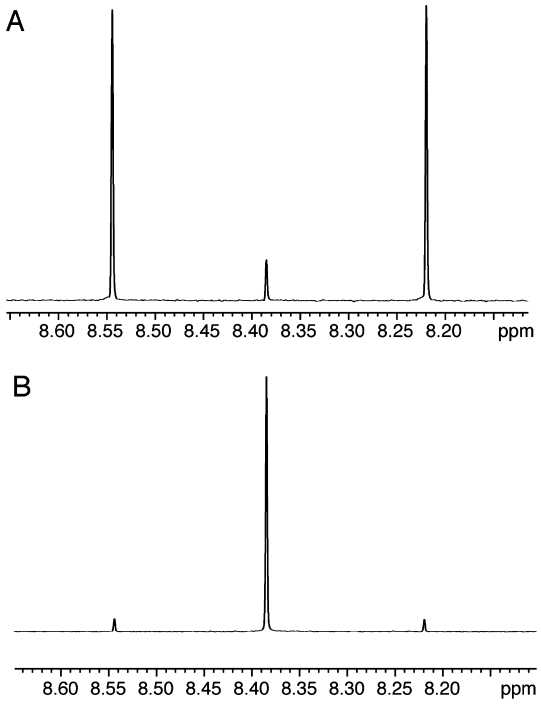

Figure 5. Downfield regions of ^{1}H NMR spectra of reaction mixtures after 3 days of reaction for **2**^{1} (A) and **2**^{2} (B) showing only signals from formate at δ = 8.385 ppm. In spectrum A, [H^{13}COO^{-}]/[H^{12}COO^{-}] ≅ 9/1; in spectrum B, this ratio is ∼1/9. In spectra A and B, $^{1}J_{CH}$ in H^{13}COO^{-} was 194.8 Hz. The ^{13}C isotope effect on δH in formate ($\delta_{13C} - \delta_{12C}$) is −1.8 Hz at 600 MHz.

pool produced from **2**^{1} contained ∼90% H^{13}COO^{-} and ∼10% H^{12}COO^{-}, whereas that produced from **2**^{2} contained ∼10% H^{13}COO^{-} and ∼90% H^{12}COO^{-}. Because these pools were generated early in the reaction before substantial degradation of **2** had taken place, the detection of substantial unlabeled formate from **2**^{1}, and substantial labeled formate from **2**^{2}, provides indirect support for the hypothesis that C1 and C2 are transposed during degradation. Experiments with doubly ^{13}C-labeled **2** were conducted to obtain more direct support for this hypothesis.

C. Degradation of D-[1,2-^{13}C$_2$]Glucosone 2^{1,2}. Studies with **2**^{1,2} were undertaken to determine the chemical fate of the C1−C2 fragment during degradation, specifically to determine the presence or absence of C1−C2 connectivity in the degradation products as detected through signal splitting from one-bond ^{13}C−^{13}C spin-coupling ($^{1}J_{CC}$).

After 1 day of reaction, H^{13}COO^{-} was detected (Figure 6). Downfield signals were observed for [1,2-^{13}C$_2$]glycolate **7**^{1,2} (doublet from the carboxyl carbon; 182.67 ppm/182.30 ppm), D-[1-^{13}C]arabinonate **6**^{1} (181.88 ppm), and H^{13}CO$_3^{-}$. The anomeric region was dominated by signals from the C1 and C2 carbons of unreacted **2**^{1,2}, with each of the eight major signals split into doublets due to $^{1}J_{C1,C2}$. The upfield region contained signals from D-[1-^{13}C]ribulose **3**^{1} (69.08, 65.45, and 65.18 ppm), [1,2-^{13}C$_2$]glycolate **7**^{1,2} (from the hydroxymethyl carbon; 64.05 ppm/63.69 ppm)), and from unidentified intermediates (∼62 ppm; ∼62.44 ppm/∼62.03 ppm). The latter signals appeared as doublets, indicating that the C1−C2 fragment from **2**^{1,2} remained intact in these species.

After 6 days of reaction, the carboxyl signal from **7**^{1,2} became more pronounced (182.67 ppm/182.30 ppm), signals from **2**^{1,2} disappeared, and the anomeric region contained signals from D-[1-^{13}C]ribose **8**^{1} and D-[1-^{13}C]arabinose **9**^{1} (Figure 7). Signals from **3**^{1} were still detected, in addition to those arising from the C2 carbon of **7** and from the unidentified intermediates. However, signals arising from the latter two species changed in character; in both cases, a new line appeared in the center of each doublet, suggesting the production of a second source of glycolate during degradation, and revealing a pool of unidentified intermediates that lacks an intact ^{13}C−^{13}C fragment. These findings show that, early in the reaction, **7** forms directly from **2**^{1,2} via C2−C3 bond cleavage, giving **7**^{1,2}, whereas later in the reaction, when the solution contains little or no **2**^{1,2}, a second source of glycolate derives from the degradation of intermediate D-[1-^{13}C]ribulose **3**^{1} via C2−C3 bond cleavage, giving **7**^{2} (i.e., these findings confirm the two routes proposed for glycolate production in Scheme 5).

After 22 days of degradation, little changed in the downfield region of the ^{13}C NMR spectrum, but the anomeric region contained new signals from D-[1-^{13}C]xylose **14**^{1} and D-[1-^{13}C]lyxose **11**^{1} (Figure S3 in Supporting Information). The upfield region also contained new signals from D-[1-^{13}C]xylulose **10**^{1}. The C2 signal of **7** appeared as a triplet due to the presence of both **7**^{1,2} and **7**^{2} in solution (Figure S4, Supporting Information). Similarly, signals from the unidentified intermediates at ∼62 ppm revealed a mixture of singly and doubly ^{13}C-labeled isotopomers. After 61 days (Figure S5, Supporting Information), signals from all four D-[1-^{13}C]-aldopentoses were observed in the anomeric region, and the upfield region was dominated by signals from [2-^{13}C]glycolate **7**^{2} (major isotopomer) and [1,2-^{13}C$_2$]glycolate **7**^{1,2} (minor isotopomer).

D. Degradation of D-[1,3-^{13}C$_2$]Glucosone 2^{1,3}. Degradation studies with **2**^{1,3} were conducted to test for the formation of D-[1,2-^{13}C$_2$]ribulose **3**^{1,2}, which is expected if C1−C2 transposition occurred during degradation. Detection of C1 signals in **3** split by the one-bond ^{13}C−^{13}C spin-coupling would provide direct evidence for this process.

After 20 days of reaction, downfield signals due to D-[2-^{13}C]ribulose **3**^{2} (keto form; 215.14 ppm) and H^{13}COO^{-} were detected (Figure 8). The dominant signals in the anomeric carbon region arose from D-[2-^{13}C]ribulose **3**^{2} (cyclic forms; 108.26 and 105.15 ppm) and unreacted **2**^{1,3} (97.66,

dx.doi.org/10.1021/ja3020296 | J. Am. Chem. Soc. 2012, 134, 11511−11524

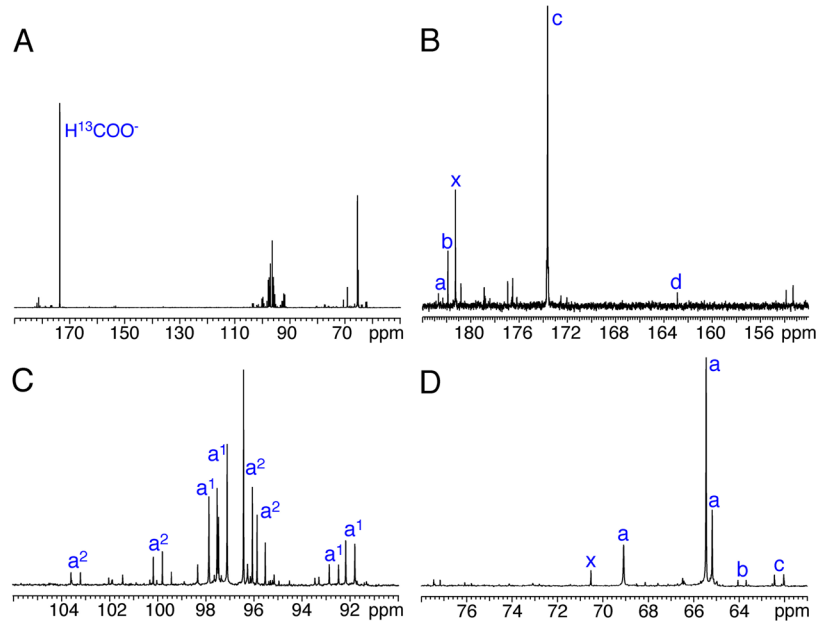

Figure 6. The $^{13}C\{^{1}H\}$ NMR spectrum of the reaction mixture with $\mathbf{2}^{1,2}$ (100 mM NaP_i; pH 7.5; 37 °C) after 1 day. (A) Full spectrum. (B) Downfield region showing weak signals from [1,2-$^{13}C_2$]glycolate $\mathbf{7}^{1,2}$ (a), D-[1-^{13}C]arabinonate $\mathbf{6}^{1}$ (b), $H^{13}COO^-$ (c), and $H^{13}CO_3^-$ (d). Signal x arises from an unidentified intermediate that disappears over time. (C) The anomeric carbon region showing signals (doublets) from C1 (a^1) and C2 (a^2) of unreacted $\mathbf{2}^{1,2}$. (D) Upfield region showing signals from D-[1-^{13}C]ribulose $\mathbf{3}^{1}$ (a), [1,2-$^{13}C_2$]glycolate $\mathbf{7}^{1,2}$ (b), and unidentified intermediates (c). Signal x was also unidentified.

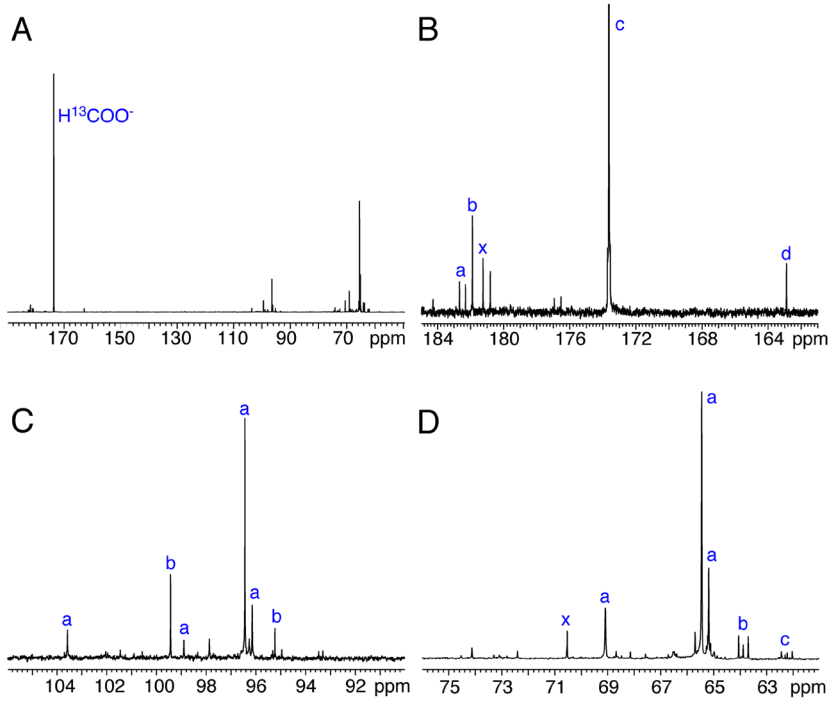

Figure 7. The $^{13}C\{^{1}H\}$ NMR spectrum of the reaction mixture with $\mathbf{2}^{1,2}$ (100 mM NaP_i; pH 7.5; 37 °C) after 6 days. (A) Full spectrum. (B) Downfield region showing weak signals from [1,2-$^{13}C_2$]glycolate $\mathbf{7}^{1,2}$ (a), D-[1-^{13}C]arabinonate $\mathbf{6}^{1}$ (b), $H^{13}COO^-$ (c), and $H^{13}CO_3^-$ (d). Signal x arises from an unidentified intermediate that disappears over time. (C) The anomeric carbon region showing signals from D-[1-^{13}C]ribose $\mathbf{8}^{1}$ (a) and D-[1-^{13}C]arabinose $\mathbf{9}^{1}$ (b). (D) Upfield region showing signals from D-[1-^{13}C]ribulose $\mathbf{3}^{1}$ (a), [1,2-$^{13}C_2$] $\mathbf{7}^{1,2}$ and [2-^{13}C]glycolate $\mathbf{7}^{2}$ (b), and unidentified intermediates (c). Signal x was also unidentified.

97.25, 92.68, and 92.01 ppm). Closer inspection of the former signals revealed the presence of weak satellites on each signal (108.43 ppm/108.08 ppm; 105.32 ppm/104.98 ppm) indicative of a minor population of D-[1,2-$^{13}C_2$]ribulose $\mathbf{3}^{1,2}$. The upfield region contained signals from D-[1,2-$^{13}C_2$]ribulose $\mathbf{3}^{1,2}$, with the C1 signals of the α- and β-furanose and keto forms split by $^{1}J_{C1,C2}$ values consistent with those reported previously in authentic **3** ($^{1}J_{C1,C2}$ (αf) = 51.8 Hz; $^{1}J_{C1,C2}$ (βf) = 51.3 Hz; $^{1}J_{C1,C2}$ (keto) = 41.5 Hz).[25] Signals from [2-^{13}C]-glycolate $\mathbf{7}^{2}$ (63.75 ppm) and unidentified intermediates (~62

dx.doi.org/10.1021/ja3020296 | J. Am. Chem. Soc. 2012, 134, 11511−11524

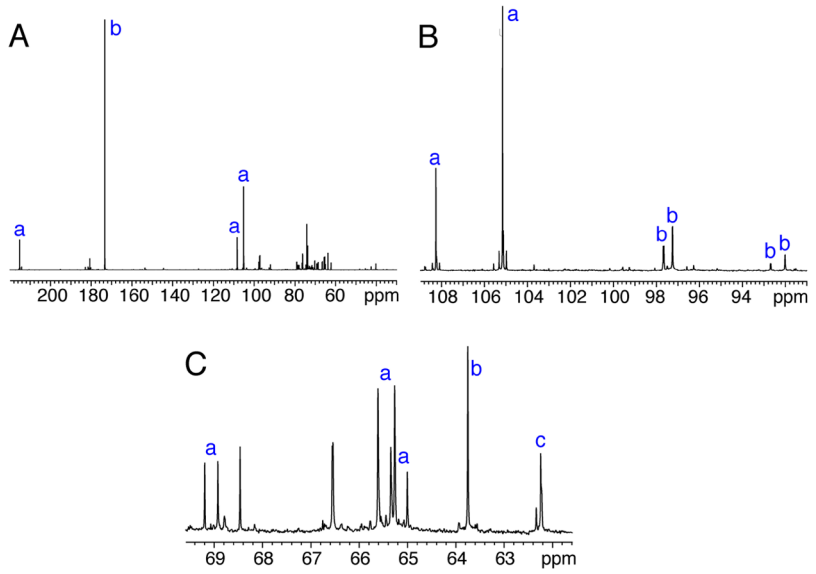

Figure 8. The $^{13}C\{^{1}H\}$ NMR spectrum of the reaction mixture with $\mathbf{2}^{1,3}$ (100 mM NaP_i; pH 7.5; 37 °C) after 20 days. (A) Full spectrum showing signals from D-[2-^{13}C]ribulose $\mathbf{3}^{2}$ (keto and furanose forms) (a) and $H^{13}COO^-$ (b). (B) The anomeric carbon region showing the C2 signals (cyclic forms) of $\mathbf{3}^{2}$ (a), D-[1,2-$^{13}C_2$]ribulose $\mathbf{3}^{1,2}$ (satellites on a), and unreacted $\mathbf{2}^{1,3}$ (b). (C) Upfield region showing signals from $\mathbf{3}^{1,2}$ (a), [2-^{13}C]glycolate $\mathbf{7}^{2}$ (b), and unidentified intermediates (c).

ppm) were also observed. After 29 days, the latter glycolate signal contained satellites attributed to the presence of a small population of [1,2-$^{13}C_2$]glycolate $\mathbf{7}^{1,2}$ (Figure 9).

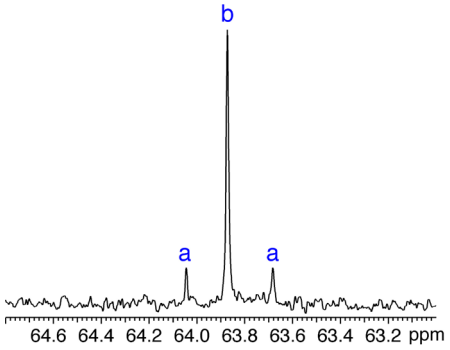

Figure 9. The C2 signals of glycolate **7** detected after 29 days of degradation of $\mathbf{2}^{1,3}$. Signals "a" arise from $\mathbf{7}^{1,2}$ and are split by $^{1}J_{C1,C2}$ = 54.7 Hz. Signal "b" at δ 63.87 ppm arises from $\mathbf{7}^{2}$. The ^{13}C isotope shift for C2 ($\delta_{C1,2} - \delta_{C2}$) is −1.4 Hz at 150 MHz.

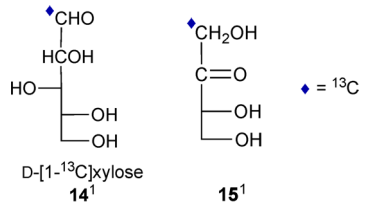

After 76 days of reaction, the C2 signals of D-[2-^{13}C]ribulose $\mathbf{3}^{2}$ and D-[2-^{13}C]xylulose $\mathbf{10}^{2}$ were observed in the anomeric carbon region of the spectrum (Figure 10). Inspection of the former signals showed them to be complex, with each composed of singlets bracketed by weak satellites. Weak singlets slightly upfield of the main singlet were also observed. These results suggest the presence of a major population of D-[2-^{13}C]ribulose $\mathbf{3}^{2}$ and a minor population of D-[1,2-$^{13}C_2$]-ribulose $\mathbf{3}^{1,2}$ in solution; the upfield weak singlets are probably produced by hydrogen−deuterium exchange with the $^{2}H_2O$ solvent (~10% $^{2}H_2O$ in $^{1}H_2O$, *v*/*v*) at sites adjacent to C2 (H1*R*/*S* and/or H3) after extended incubation, which would cause small upfield shifts in the C2 signal. The upfield region is similar to that in Figure 8, although the [2-^{13}C]glycolate signal now dominated those from $\mathbf{3}^{1,2}$, and weak satellites on the C2 signal of $\mathbf{7}^{2}$ were still observable, indicating the presence of [1,2-$^{13}C_2$]glycolate $\mathbf{7}^{1,2}$. In summary, the key finding from the degradation studies of $\mathbf{2}^{1,3}$ is that D-[1,2-$^{13}C_2$]ribulose $\mathbf{3}^{1,2}$ is produced, thus providing key confirmatory evidence that C1−C2 transposition occurred during the degradation (Scheme 7).

E. Degradation of D-[1-^{13}C]Xylosone $\mathbf{5}^{1}$. The degradation of D-[1-^{13}C]xylosone $\mathbf{5}^{1}$ (D-[1-^{13}C]*threo*-pentos-2-ulose) was investigated to determine whether this structurally related C_5 osone degrades in a manner similar to that of **2**. The $^{13}C\{^{1}H\}$ NMR spectrum of the reaction mixture after 2 days (Figure S6, Supporting Information) showed an intense signal from $H^{13}COO^-$ (173.62 ppm), and essentially no unreacted $\mathbf{5}^{1}$ was detected. The upfield region contained signals from [2-^{13}C]glycolate $\mathbf{7}^{2}$ (63.88 ppm) and from unidentified intermediates having chemical shifts (~62 ppm) similar to those observed in reactions with $\mathbf{2}^{1}$. Importantly, signals from C1 (68.48 ppm), C3 (78.51 ppm), and C4 (65.56 ppm) of the predominant keto form of $\mathbf{15}^{1}$ were also observed,[27] with that from C1 considerably more intense than those from C3 and C4, suggesting that D-[1-^{13}C]erythrulose $\mathbf{15}^{1}$ formed during the reaction. Glycolate $\mathbf{7}^{2}$ presumably arises from C2−C3 bond cleavage of $\mathbf{15}^{1}$, analogous to the behavior of $\mathbf{3}^{1}$ (Scheme 5). These findings demonstrate that C1−C2 transposition detected during the degradation of **2** is not unique to this C_6 osone but instead may be a general characteristic of osone degradation when C3 bears an hydroxyl substituent.

F. The Effect of Buffer on the Degradation Rates of 2. A potential role of the buffer in the degradation of **2** was investigated by comparing the reaction rate in 100 mM phosphate buffer (pH 7.5) at 37 °C with those observed in no buffer (pH 9.5, solution pH adjusted with NaOH), in 400 mM phosphate buffer (pH 7.5), in 100 mM MOPS buffer (pH 7.5),

dx.doi.org/10.1021/ja3020296 | J. Am. Chem. Soc. 2012, 134, 11511−11524

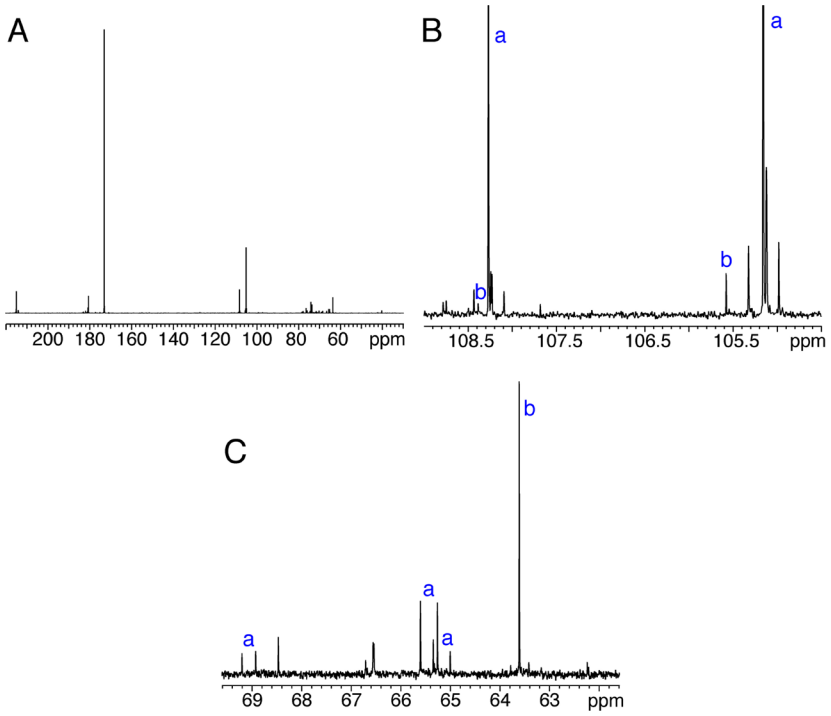

Figure 10. The $^{13}C\{^1H\}$ NMR spectrum of the reaction mixture with **2**[1,3] (100 mM NaP_i; pH 7.5; 37 °C) after 76 days. (A) Full spectrum. (B) The anomeric carbon region showing the C2 signals of D-[2-^{13}C]ribulose **3**[2] (a; signal intensities are off-scale) and D-[1,2-$^{13}C_2$]ribulose **3**[1,2] (satellites). Note the weak singlets slightly upfield of the central signal, which are probably due to **3** containing ^{2}H at H1 and/or H3. D-[2-^{13}C]Xylulose **10**[2] is also detected (b). (C) Upfield region showing signals from **3**[1,2] (a) and [2-^{13}C]glycolate **7**[2] (b). The weak satellites bracketing the latter signal indicate the presence of [1,2-$^{13}C_2$]glycolate **7**[1,2] in the solution.

Scheme 7

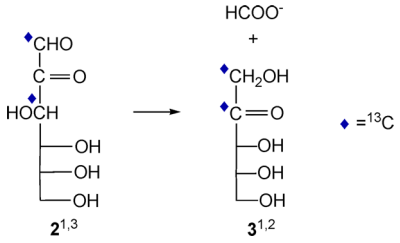

and in 100 mM sodium citrate buffer. In the absence of buffer at pH 9.5, little if any degradation occurred after 36 days (Figure S7, Supporting Information), even though the solution pH was three units higher than that of the standard phosphate buffer used in this investigation. Aqueous solutions of **2** appear to be very stable at elevated temperatures and moderately alkaline conditions. These findings suggested that phosphate may play a role in catalyzing the degradation of **2**.

Reactions conducted in the MOPS and citrate buffers gave degradation rates similar to that found with no buffer. However, when 400 mM phosphate buffer was employed, the degradation rate increased significantly relative to that found in 100 mM phosphate buffer.

Trace metals are common contaminants in commercial sources of sodium phosphate and thus could be responsible for the observed rate enhancements in phosphate buffer. However, the reaction rate in 100 mM phosphate containing 5 mM EDTA was the same as that in 100 mM phosphate, providing further evidence that phosphate plays a specific role in catalyzing the degradation of **2**.

Given the findings in phosphate buffer, a reaction was conducted in 100 mM sodium arsenate (pH 7.5) at 37 °C, because arsenate often behaves as a phosphate surrogate in chemical and biochemical structures and transformations.[28] Under these solution conditions, the degradation reaction proceeded rapidly and gave time-lapse NMR data similar to those obtained with phosphate buffer (Figure S8, Supporting Information).

G. Degradation of DL-[1-^{13}C]Glyceraldehyde 4[1]. $^{13}C\{^1H\}$ NMR results from the degradation of different ^{13}C-isotopomers of **2** confirm that an early and major intermediate is D-ribulose **3**. However, the generation of **3** from **2** does not occur exclusively by direct C1−C2 bond cleavage as shown in Scheme 3. In addition to this route, degradation is accompanied by C1−C2 transposition ~10% of the time based on NMR signal integrations (Figure 5). Once **3** forms, it undergoes further cleavage to give glycolate **7**, with the C1 and C2 carbons of **7** arising from C2 and C1, respectively, of **3** (Scheme 5). This cleavage may give D-glyceraldehyde **4** as the C_3 byproduct. ^{13}C NMR evidence for the transient formation of **4** at low concentrations was obtained (from experiments with **2**[4]; data not shown); **4** never accumulates in the reaction mixture, presumably due to its lability under the reaction conditions (i.e., its steady-state concentration is very low). The potential contribution of **4** to the degradation profile of **2** was investigated by examining the degradation of authentic DL-[1-^{13}C]glyceraldehyde **4**[1] in 100 mM phosphate buffer at pH 7.5 and 37 °C (Figure S9, Supporting Information). After one day, most of **4**[1] had isomerized to [1-^{13}C]dihydroxyacetone **16**[1] ([1-^{13}C]1,3-dihydroxypropanone); the aldose−ketose equilibrium favors the keto form under these conditions (Scheme 8) (Figure S9B).[29] Ketose **16**[1] undergoes subsequent degradation to yield [^{13}C]formate and [2-^{13}C]glycolate **7**[2], presumably via C1−C2 cleavage similar to what occurs in 2-ketopentose **3**

dx.doi.org/10.1021/ja3020296 | J. Am. Chem. Soc. 2012, 134, 11511−11524

Scheme 8

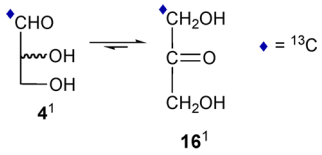

(Figure S9C) (Scheme 5). These results confirm that **4** is unstable under the solution conditions used for the degradation of **2**, thus explaining its lack of accumulation in the reaction mixture.

CONCLUSIONS

The degradation of D-glucosone **2** in aqueous phosphate buffer (pH 7.5, 37 °C) occurs by a series of reactions distinctly different from that reported recently for 3-deoxy-D-glucosone **1**.[17] Unlike **1**, osone **2** does not undergo carbon skeleton rearrangement via intramolecular 1,2-hydrogen transfer to any appreciable extent; neither D-gluconate **12** nor D-mannonate **13** could be detected in reaction mixtures. Instead, two backbone fragmentation events are favored early in the degradation: C1−C2 cleavage to give formate and D-ribulose **3**, and C2−C3 cleavage to give glycolate and an unidentified C_4 byproduct, possibly D-erythrose or D-erythrulose. The D-ribulose intermediate is susceptible to further degradation, which occurs primarily by C2−C3 cleavage to give glycolate and a C_3 byproduct, possibly D-glyceraldehyde or dihydroxyacetone. Thus, in **2**, degradation occurs primarily via backbone fragmentation into 1- (formate) or 2- (glycolate) carbon units; this behavior may have practical implications in the conversion of sugar feedstocks to useful chemical precursors and end-products. The identification of 2-ketopentose **3** as the initially formed major degradation intermediate confirms prior claims made by Baynes and co-workers,[24] and the NMR studies with ^{13}C-labeled substrates lead to a mechanism for its formation (Scheme 3). The degradation of the C_3 and C_4 byproducts generated from these C−C bond cleavage events was not investigated here.

The production of D-ribulose **3** from D-glucosone **2**, however, does not occur exclusively by the mechanism shown in Scheme 3. If this mechanism were sufficient to account for all conversions of **2** to **3**, then $\mathbf{2}^1$ and $\mathbf{2}^2$ would yield only **3** and $\mathbf{3}^1$, respectively. The experimental data suggest otherwise. NMR data obtained from the degradation of $\mathbf{2}^1$, $\mathbf{2}^2$, $\mathbf{2}^{1,2}$, and $\mathbf{2}^{1,3}$, interpreted collectively, lead to the internally consistent conclusion that the conversion can be accompanied by C1−C2 transposition; for example, during the degradation of $\mathbf{2}^{1,3}$, two ^{13}C-isotopomers of **3** are produced, $\mathbf{3}^2$ and $\mathbf{3}^{1,2}$ (Scheme 9). Partitioning between these two ^{13}C isotopomers is not equal; ∼90% of $\mathbf{2}^{1,3}$ converts to $\mathbf{3}^2$, and ∼10% converts to $\mathbf{3}^{1,2}$. C1−C2 transposition is a minor event but its occurrence is nevertheless remarkable and unexpected. Furthermore, this transposition does not appear to be unique to **2**, because D-xylosone **5** behaves similarly. It is thus likely that most, if not all, 1,2-dicarbonyl sugars containing a hydroxyl group at C3 undergo the same rearrangement. 1,2-Dicarbonyl sugars containing this consensus C1−C3 backbone substructure possess a latent ability to undergo C1−C2 transposition during degradation.

The detection of C1−C2 transposition led to investigations of the potential role of phosphate as a mediator of osone degradation and/or C1−C2 transposition. While an exhaustive

Scheme 9

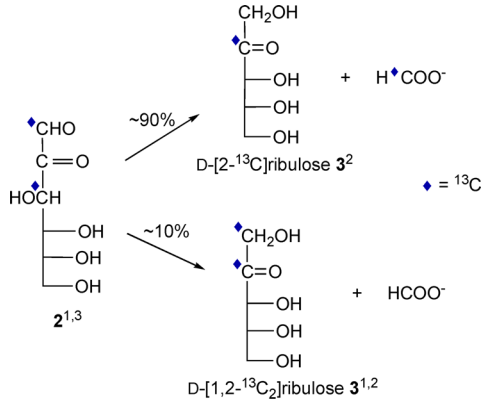

set of buffers was not examined, the present findings show that inorganic phosphate (P_i), and the P_i surrogate, arsenate, catalyze the degradation of 1,2-dicarbonyl sugars. Aqueous solutions of **2** at moderately alkaline pH that are devoid of buffer species are very stable, even at 37 °C. These findings imply that **2** generated under in vivo conditions most likely degrades via a P_i-catalyzed mechanism.

C1−C2 transposition during carbohydrate transformations, although rare, has been documented previously, most notably in the molybdate-catalyzed epimerization of aldoses (Scheme 10).[30] In the latter process, dimolybdate is believed to bind

Scheme 10

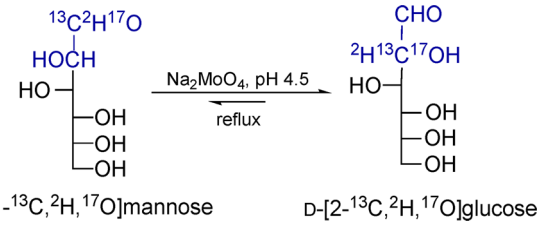

reversibly to the acyclic hydrate (1,1-*gem*-diol) form of an aldose substrate, and this complex promotes C2-epimerization with concomitant C1−C2 transposition, doing so in a stereospecific manner. Using this reaction as a model, possible mechanistic explanations of the observed C1−C2 transposition during the degradation of **2** were considered that involve putative transient and reversible P_i adducts with the osone. In doing so, an implicit assumption was made that not only does P_i catalyze the overall rate of degradation, but it is also associated with the concomitant C1−C2 transposition. Because the rate of degradation of **2** is very low in the absence of P_i, it remains unclear whether C1−C2 transposition occurs under these solution conditions. Efforts were not made to conduct degradation reactions over extended time periods to address this question.

With the above caveats in mind, it is self-evident that the significantly different pathways of degradation of **1** and **2** can be attributed to differences in covalent structure at C3. The presence of a C3 hydroxyl group *α* to the C2 carbonyl renders H3 considerably more acidic in **2** than are either H3*R* or H3*S* in **1**. The reduced H3 acidities in **1** presumably render C1−C2 cleavage and/or 1,2-hydrogen transfer[17] more favored than enolization and subsequent rearrangement. Thus, a useful starting point for considering how P_i-mediated C1−C2

dx.doi.org/10.1021/ja3020296 | J. Am. Chem. Soc. 2012, 134, 11511−11524

Scheme 11

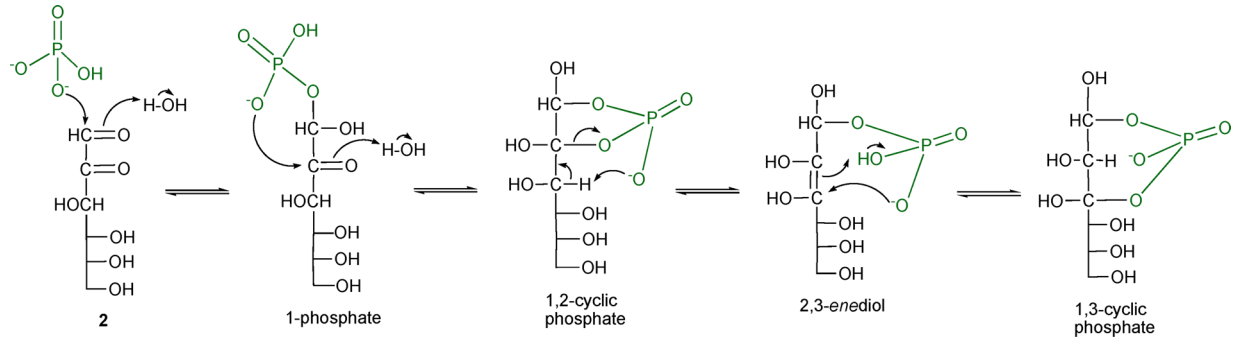

transposition might occur would be H3 abstraction and subsequent enolization at C3.

Potential ways by which P_i might form reversible adducts with osone **2** were considered based on prior substrate specificity studies of the enzyme, glycerol kinase (GK) (EC 2.7.1.30) (Scheme S3, Supporting Information).[31] Both L-glyceraldehyde and D-glyceraldehde bind to GK, but only the former is phosphorylated to give L-glyceraldehyde 3P. When D-glyceraldehde is the substrate, GK behaves like an ATPase, presumably because phosphorylation occurs at one of the C1 hydroxyl groups of the putative bound 1,1-*gem*-diol form of the substrate. Release of this phosphorylated product by GK is followed by rapid hydrolysis in solution to give P_i and the original starting triose. In this mechanism, P_i is transiently bonded to a hemiacetal hydroxyl group, and this ester bond is readily hydrolyzed in solution. Similar adducts thus appeared to be reasonable intermediates in the P_i-mediated degradation of **2**.

The above considerations led to a mechanism for the conversion of osone **2** to ketose **3** involving P_i as a catalyst at pH 7.5 (Scheme 11). Osone **2** reacts with P_i to give a 1-phosphate adduct, which then cyclizes to give a 1,2-cyclic phosphate intermediate (formation of the 2-phosphate could also occur first). Adduct formation is favorable, because C1 and C2 are electrophilic and thus susceptible to nucleophilic attack by P_i. The intermediate 1,2-cyclic phosphate is now activated for enolization, because abstraction of the relatively acidic H3 is promoted by the proximal bound phosphate monoanion to give the 2,3-enediol. Subsequent rearrangement of the latter gives a 1,3-cyclic phosphate, which can undergo hydrolysis to give an unphosphorylated 1,3-dicarbonyl intermediate and P_i. The phosphorylated 1,3-dicarbonyl intermediate (or its unphosphorylated equivalent) is postulated to be the key intermediate in subsequent chemical transformations.

The 1,3-cyclic phosphate serves as an intermediate in the formation of **3** (Scheme 12). Attack by OH^- at C1, with concomitant cleavage of the C1−C2 bond, gives an intermediate with the phosphate group tethered to the chemical equivalents of formate and **3**. Subsequent hydrolysis gives the free ketose **3** after dehydration. Alternatively, OH^- attack at C1 of the 1,3-cyclic phosphate and C1−C2 bond cleavage could produce a untethered C1−C2 enediol intermediate (phosphate serves as the leaving group) that undergoes isomerization to give D-ribulose (also giving D-ribose and D-arabinose). The free 1,3-dicarbonyl sugar (see above) may also serve as a substrate in the reaction sequence, in this case undergoing attack by OH^- to give **3** and formate directly.

The free 1,3-dicarbonyl intermediate, derived from hydrolysis of the 1,3-cyclic phosphate in Scheme 11, is implicated in the formation of glycolate from **2** (Scheme 13). Abstraction of the acidic H2 generates a conjugated 1,2-enediol-3-keto intermediate, which subsequently enolizes to a 2,3-dicarbonyl intermediate. Cleavage of the C2−C3 bond in the latter, promoted by OH^-, gives glycolate **7** and D-erythrose. This mechanism explains the formation of **7**[1] from **2**[2] (Scheme 5).

Scheme 12

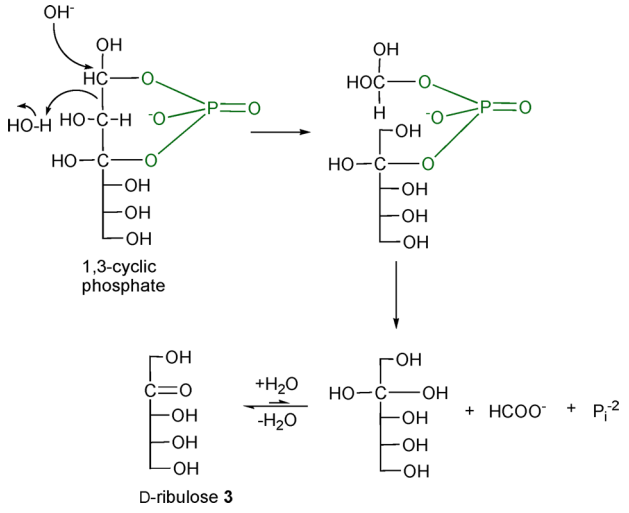

Scheme 13

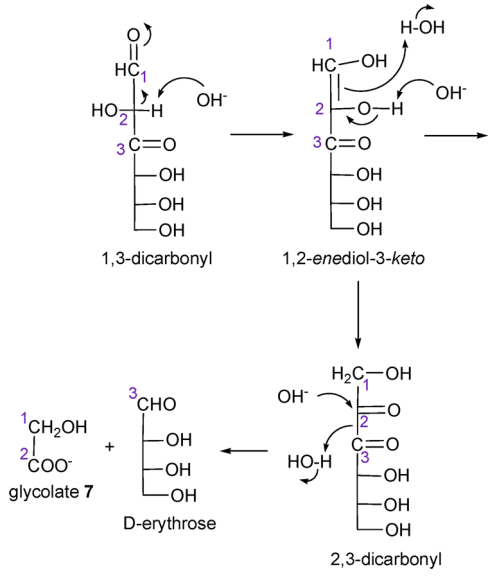

dx.doi.org/10.1021/ja3020296 | J. Am. Chem. Soc. 2012, 134, 11511−11524

Scheme 14

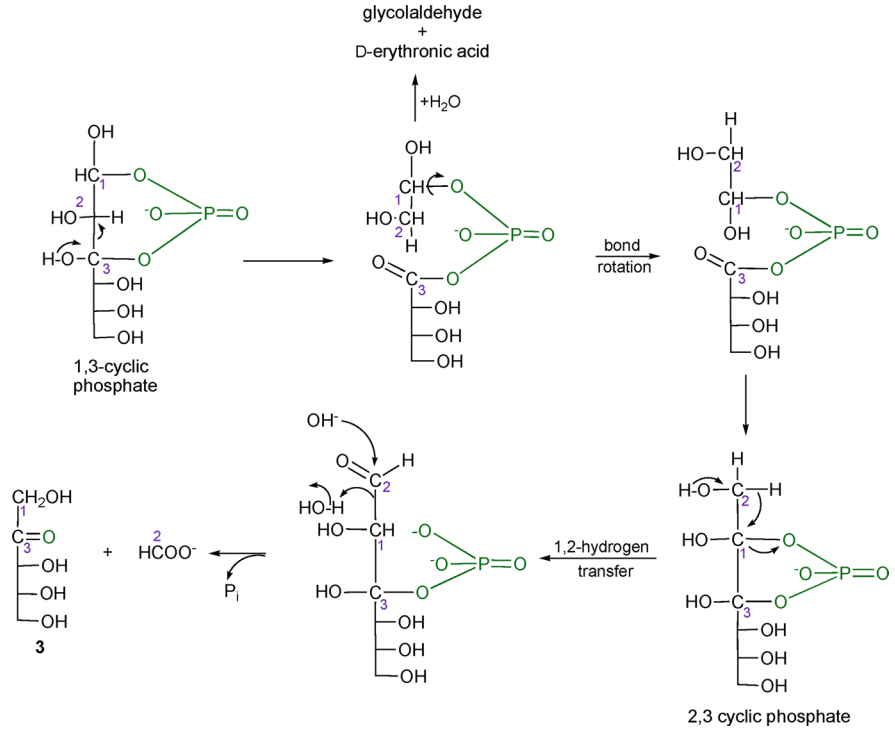

Scheme 15

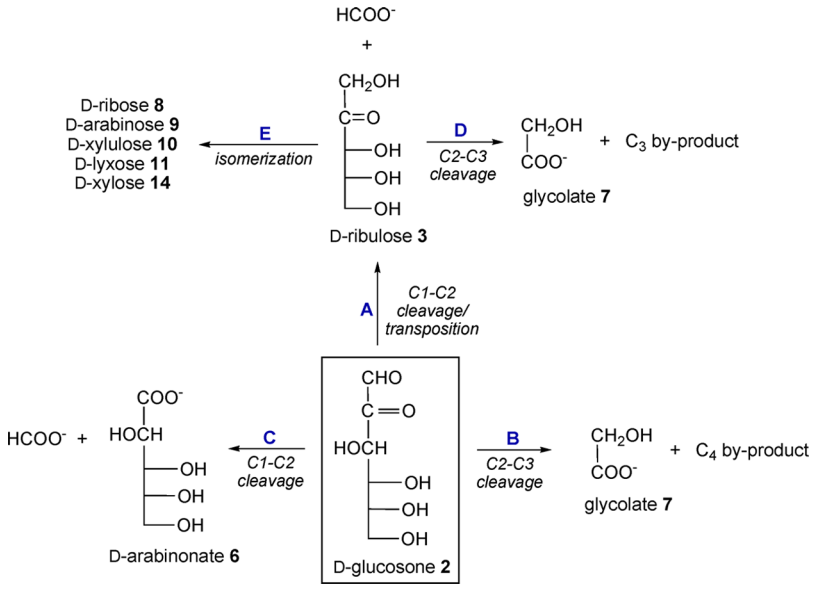

In summary, the mechanism shown in Scheme 11 explains the observed catalysis by P_i in the degradation of **2** and implicates a 1,3-cyclic phosphate intermediate. The latter phosphate, or the free 1,3-dicarbonyl sugar derived from it, rearranges to D-ribulose (Scheme 12). The 1,3-dicarbonyl intermediate is also implicated in the formation of **7** from **2** (Scheme 13). Approximately 90% of **2** degrades through these routes based on the results of ^{13}C-labeling studies. The remaining 10% of **2** follows a different route responsible for the observed C1−C2 transposition.

A potential mechanism for C1−C2 transposition is initiated with the 1,3-cyclic phosphate intermediate, which undergoes C2−C3 bond cleavage (retro-aldol-like) to give phosphate-tethered C_2 and C_4 fragments (Scheme 14). After bond rotation, the latter are rejoined at C1 and C3 (aldol-like condensation). An internal redox reaction involving 1,2-hydrogen transfer (analogous to what is observed during the degradation of **1**)[17] gives the 1,3-dicarbonyl intermediate, which undergoes OH^--mediated C1−C2 bond cleavage to give **3** and formate. The key transformation in this mechanism is the 1,2-hydrogen transfer that occurs after bond rotation and the aldol-like condensation.

In an alternate mechanism, the tethered C1−C2 fragment (glycolaldehyde) in Scheme 14 can lose water to give a tethered enediol fragment, with subsequent transfer of phosphate to the equivalent C2 hydroxyl. Addition of water gives the original two

dx.doi.org/10.1021/ja3020296 | J. Am. Chem. Soc. 2012, 134, 11511−11524

carbon fragment in which C1 and C2 have been inverted. Condensation to the original C3 leads to 3 containing the original C1 of the 1,3-cyclic phosphate at C1 of the ketose. This alternate mechanism for C1−C2 transposition eliminates the need for a 1,2-hydrogen transfer step in Scheme 14.

The proposed mechanisms shown in Schemes 11−14 involve P_i in various saccharide adducts during the degradation of **2**. In these mechanisms, P_i is covalently attached to reaction intermediates either via an ester bond to a hemiacetal/hemiketal hydroxyl group or via a mixed anhydride bond to a carboxylic acid. These attachments allow facile hydrolysis to liberate P_i when the rearrangement is complete. Potential mechanisms in which P_i is attached via ester linkage to a primary or secondary hydroxyl group were excluded; these bonds are relatively stable, would presumably hydrolyze slowly under the reaction conditions, and would be expected to accumulate during the reaction. NMR studies showed no evidence of stable phosphorylated intermediates or end-products; the latter would have been suggested from the observation of $^{13}C-^{31}P$ spin-coupling when the ^{31}P atom is two- or three-bonds removed from the carbon under observation.[32]

The competing degradation routes for **2** in aqueous phosphate buffer are summarized in Scheme 15. Pathways A, B, and C consume **2**, with pathway A involving C1−C2 bond cleavage with or without C1−C2 transposition to give D-ribulose **3** and formate. A second C1−C2 bond cleavage mode (pathway C) gives D-arabinonate **6** and formate. The third pathway (B) involves C2−C3 bond cleavage to give glycolate **7** and a C_4 byproduct. Two secondary degradation pathways emanate from intermediate **3**. Pathway D involves C2−C3 bond cleavage to give glycolate **7** and a C_3 byproduct, and pathway E involves isomerization to give the four D-aldopentoses (**8**, **9**, **11**, **14**) and D-xylulose **10**. In the present work, reaction mixtures were not incubated for more than ∼90 days, and thus additional degradation pathways may exist in more prolonged incubations.

The observation that ∼10% of **2** undergoes C1−C2 transposition during degradation leads to the question of whether this transposition could be made more favorable. If the mechanisms in Scheme 12 and 14 are correct, how might the C2−C3 bond cleavage (retro-aldol-like) reaction be made more favorable than C1−C2 bond cleavage? Might, for example, the presence of an electronegative substituent such as fluorine at C4 of the starting osone (e.g., 4-fluoro-D-glucosone) promote C2−C3 bond cleavage over C1−C2 bond cleavage? A equally intriguing question is whether 1,2-dicarbonyl sugars undergo C1−C2 transposition in vivo, presumably involving P_i catalysis. Answers to these questions invite further study.

The mechanisms shown in Schemes 11−14 could be tested in at least two ways. Preparation of the proposed 1,3-dicarbonyl intermediate, 3-keto-D-glucose (by C3 oxidation and deprotection of 1,2;5,6-di-*O*-isopropylidene-α-D-glucofuranose[33]), and investigations of its degradation in the presence and absence of P_i might shed light on its putative central role in the degradation of **2**. In addition, NMR studies with $^2H/^{13}C$ doubly labeled **2** could prove useful to test the mechanism shown in Scheme 14 in which 1,2-hydrogen transfer is implicated. These, and other experiments, will be the subjects of future reports.

The primary motivation for conducting this work was mechanistic, namely, to examine the effect of C3 structure on the degradation of 1,2-dicarbonyl sugars; the unusual backbone rearrangement that occurred was unanticipated. The implications of these findings for human health, especially for diabetes, are at least 2-fold. The steady-state concentration of **2** in vivo under diabetic conditions is not well established, but it is probably lower than that of **1**. The extent to which **2** reacts with proteins in vivo is unclear, although its *intrinsic* reactivity relative to **1** is probably higher (greater electrophilic character at C2). Future in vivo metabolic studies involving the use of isotopically labeled **2** must now include the possibility of C1−C2 transposition when establishing the fates of specific labeled carbons; a simple backbone degradation pathway cannot be assumed. The present work was conducted in vitro under phosphate-buffered and temperature conditions that only crudely approximate those in vivo, and thus it would be worthwhile conducting degradation studies in plasma or other biological media to test whether the degradation route is affected, especially with respect to the C1−C2 transposition component. Second, the degradation of **2** is accompanied by the formation of multiple degradation products, including formate, glycolate, and possibly glyceraldehyde, which themselves may affect physiological function. While some of these byproducts are probably harmless when generated sporadically, long-term chronic exposure to them in the diabetic condition may lead to metabolic aberrations not fully appreciated at the present time.

■ ASSOCIATED CONTENT

Supporting Information

Scheme S1, general scheme of protein glycation via the Amadori pathway; Scheme S2, synthesis of ^{13}C-labeled D-glucosones; Scheme S3, action of glycerol kinase on D- and L-glyceraldehyde; Figure S1, $^{13}C\{^1H\}$ NMR spectrum of the reaction mixture with **2**[2] (100 mM NaP_i; pH 7.5; 37 °C) after 50 days; Figure S2, $^{13}C\{^1H\}$ NMR spectra of reaction mixtures with D-[1-^{13}C]ribulose **3**[1] (100 mM NaP_i; pH 7.5; 37 °C); Figure S3, $^{13}C\{^1H\}$ NMR spectrum of the reaction mixture with **2**[1,2] (100 mM NaP_i; pH 7.5; 37 °C) after 22 days; Figure S4, expansion of the ^{13}C NMR spectrum shown in Figure S3; Figure S5, $^{13}C\{^1H\}$ NMR spectrum of the reaction mixture with **2**[1,2] (100 mM NaP_i; pH 7.5; 37 °C) after 61 days; Figure S6, $^{13}C\{^1H\}$ NMR spectrum of the reaction mixture with **5**[1] (100 mM NaP_i; pH 7.5; 37 °C) after 2 days; Figure S7, $^{13}C\{^1H\}$ NMR spectrum of the reaction mixture with **2**[1] after 36 days at pH 9.5 (adjusted with NaOH) and 37 °C; Figure S8, $^{13}C\{^1H\}$ NMR spectrum of the reaction mixture with **2**[1] (100 mM sodium arsenate; pH 7.5; 37 °C) after 4 days; Figure S9, degradation of D-[1-^{13}C]glyceraldehyde **4**[1] in 100 mM phosphate buffer, pH 7.5, at 37 °C; Figure S10, standard $^{13}C\{^1H\}$ NMR spectrum of sodium D-arabinonate **6** in 100 mM NaP_i buffer at pH 7.5 and 22 °C; Figure S11, standard $^{13}C\{^1H\}$ NMR spectrum of sodium glycolate **7** in 100 mM NaP_i buffer at pH 7.5 and 22 °C; Figure S12, standard $^{13}C\{^1H\}$ NMR spectrum of D-erythrulose **15** in 100 mM NaP_i buffer at pH 7.5 and 22 °C. This material is available free of charge via the Internet at http://pubs.acs.org.

■ AUTHOR INFORMATION

Corresponding Author

aseriann@nd.edu

Notes

The authors declare no competing financial interest.

■ ACKNOWLEDGMENTS

This work was supported by the National Institute of Diabetes and Digestive and Kidney Disease (DK065138).

■ REFERENCES

(1) Wild, S.; Roglic, G.; Green, A.; Sicree, R.; King, H. *Diabetes Care* **2004**, *27*, 1047−1053.
(2) Bolen, S.; Feldman, L.; Vassy, J.; Wilson, L.; Yeh, H.-C.; Marinopoulos, S.; Wiley, C.; Selvin, E.; Wilson, R.; Bass, E. B.; Brancati, F. L. *Ann. Intern. Med.* **2007**, *147*, 386−399.
(3) Kuroda, M.; Bujo, H.; Aso, M.; Saito, Y. *J. Diabetes Invest.* **2011**, *2*, 333−340.
(4) Santamaria, X.; Massasa, E. E.; Feng, Y.; Wolff, E.; Taylor, H. S. *Mol. Ther.* **2011**, *19*, 2065−2071.
(5) Zhang, Q.; Ames, J. M.; Smith, R. D.; Baynes, J. W.; Metz, T. O. *J. Proteome Res.* **2009**, *8*, 754−769.
(6) Voziyan, P. A.; Khalifah, R. G.; Thibaudeau, C.; Yildiz, A.; Jacob, J.; Serianni, A. S.; Hudson, B. G. *J. Biol. Chem.* **2003**, *278*, 46616−46624.
(7) Chetyrkin, S. V.; Mathis, M. E.; Ham, A.-J.; Hachley, D. L.; Hudson, B. G.; Voziyan, P. A. *Free Red. Biol. Med.* **2008**, *44*, 1276−1285.
(8) Ulrich, P.; Cerami, A. *Recent Prog. Hormone Res.* **2001**, *56*, 1−22.
(9) Degenhardt, T. P.; Alderson, N. L.; Arrington, D. D.; Beattie, R. J.; Basgen, J. M.; Steffes, M. W.; Thorpe, S. R.; Baynes, J. W. *Kidney Int.* **2002**, *61*, 939−950.
(10) House, A. A.; Eliasziw, M.; Cattran, D. C.; Churchill, D. N.; Oliver, M. J.; Fine, A.; Dresser, G. K.; Spence, J. D. *JAMA* **2010**, *303*, 1603−1609.
(11) Chetyrkin, S.; Mathis, M.; Pedchenko, V.; Sanchez, O. A.; McDonald, W. H.; Hachey, D. L.; Madu, H.; Stec, D.; Hudson, B.; Voziyan, P. *Biochemistry* **2011**, *50*, 6102−6112.
(12) Thornally, P. J.; Langborg, A.; Minhas, H. S. *Biochem. J.* **1999**, *344*, 109−116.
(13) Zyzak, D. V.; Richardson, J. M.; Thorpe, S. R.; Baynes, J. W. *Arch. Biochem. Biophys.* **1995**, *316*, 547−554.
(14) Szwergold, B. S.; Howell, S.; Beisswenger, P. J. *Diabetes* **2001**, *50*, 2139−2147.
(15) Nagai, R.; Unno, Y.; Hayashi, M. K.; Masuda, S.; Hayase, F.; Kinae, N.; Horiuchi, S. *Diabetes* **2002**, *51*, 2833−2839.
(16) Chetyrkin, S. V.; Zhang, W.; Hudson, B. G.; Serianni, A. S.; Voziyan, P. A. *Biochemistry* **2008**, *47*, 997−1006.
(17) Zhang, W.; Carmichael, I.; Serianni, A. S. *J. Org. Chem.* **2011**, *76*, 8151−8158.
(18) Giffhorn, F.; Köpper, S.; Huwig, A.; Freimund, S. *Enzyme Microb. Technol.* **2000**, *27*, 734−742.
(19) Freimund, S.; Huwig, A.; Giffhorn, F.; Köpper, S. *Chem.—Eur. J.* **1998**, *4*, 2442−2455.
(20) Angyal, S.; Bethell, G. S.; Beveridge, R. *Carbohydr. Res.* **1979**, *73*, 9−18.
(21) Tropper, F. D.; Andersson, F. O.; Grand-Maitre, C.; Roy, R. *Carbohydr. Res.* **1992**, *229*, 149−154.
(22) Freimund, S.; Baldes, L.; Huwig, A.; Giffhorn, F. *Carbohydr. Res.* **2002**, *337*, 1585−1587.
(23) Vuorinen, T.; Serianni, A. S. *Carbohydr. Res.* **1990**, *207*, 185−210.
(24) Wells-Knecht, K. J.; Zyzak, D. V.; Litchfield, J. E.; Thorpe, S. R.; Baynes, J. W. *Biochemistry* **1995**, *34*, 3702−3709.
(25) Vuorinen, T.; Serianni, A. S. *Carbohydr. Res.* **1990**, *209*, 13−31.
(26) (a) Drew, K. N.; Zajicek, J.; Bondo, G; Bose, B.; Serianni, A. S. *Carbohydr. Res.* **1998**, *307*, 199−209. (b) King-Morris, M. J.; Serianni, A. S. *J. Am. Chem. Soc.* **1987**, *109*, 3501−3508.
(27) The ^{13}C NMR signals for D-[1-^{13}C]erythrulose **15**[1] were assigned based on spectral data obtained from a commercial (Sigma) unlabeled sample of **15**. The following ^{13}C NMR signal assignments (in ppm) were made in 100 mM NaP_i buffer, pH 7.5, 9/1 *v*/*v* $^1H_2O/^2H_2O$, 200 mM in **15**, 22 °C: C1 (keto), 68.48; C1 (hydrate), 66.73; C2 (keto), 215.00; C2 (hydrate), 98.47; C3 (keto), 78.51; C3 (hydrate), 76.10; C4 (keto), 65.56; C4 (hydrate), 64.28. Under these solution conditions, the keto/hydrate ratio is ∼92/8.
(28) Tawfik, D. S.; Viola, R. E. *Biochemistry* **2011**, *50*, 1128−1134.
(29) Davis, L. *Bioorg. Chem.* **1973**, *2*, 197−201.
(30) (a) Hayes, M. L.; Pennings, N. J.; Serianni, A. S.; Barker, R. *J. Am. Chem. Soc.* **1982**, *104*, 6764−6769. (b) Zhao, S.; Petrus, L.; Serianni, A. S. *Org. Lett.* **2001**, *3*, 3819−3822.
(31) Hayashi, S.; Lin, E. C. C. *J. Biol. Chem.* **1967**, *242*, 1030−1035.
(32) Serianni, A. S.; Pierce, J.; Barker, R. *Biochemistry* **1979**, *18*, 1192−1199.
(33) Morris, P. E., Jr.; Hope, K. D.; Kiely, D. E. *J. Carbohydr. Chem.* **1989**, *8*, 515−530.